Supplementary Information (SI) for Physical Chemistry Chemical Physics.

Supporting Information for Astrochemical Modeling of the Propargyl Radical in TMC-1

Alex N. Byrne,*,† Ci Xue,† Troy Van Voorhis,† and Brett A. McGuire†,‡

†*Department of Chemistry, Massachusetts Institute of Technology, Cambridge, MA 02139, USA*

‡*National Radio Astronomy Observatory, Charlottesville, VA 22903, USA*

E-mail: lxbyrne@mit.edu

S1: One-at-a-time Analysis with Order of Magnitude Variation

In Figure S1 the results of an additional one-at-a-time analysis with a factor of 10 variation are shown. This analysis was performed identically to the factor of 2 variation analysis, but with 20 change factors equally spaced in log scale between 0.1 and 10. These key reaction lists agree well with those obtained with a factor of 2 variation, with slight differences in ordering as well as a few new reactions. In particular, cosmic-ray dissociation and dissociative ionization of H_2 become important to the overall network and the cosmic-ray ionization of He becomes important to $C_{10}H_7CN$ with a factor of 10 variation in rate coefficient. Additionally, the agreement between the three OAT metrics worsens with this larger range of variation, particularly for the key reactions of $C_{10}H_7CN$.

In Figure S2, abundances of $C_{10}H_7CN$ at 541100 years as a function of change in rate coefficient are shown for its key reactions according to this analysis and the RSD metric. The top 2 reactions, $C_6H_5 + CH_2CHC_2H \longrightarrow H + C_{10}H_8$ and $CH_4 + C_5H_2{}^+ \longrightarrow H + C_6H_5{}^+$, appear to have a roughly linear relationship between $C_{10}H_7CN$ abundance and factor of change in rate coefficient. Likewise, similar behavior is observed at larger factors of change for the rank 5 and 8 reactions, the reactions of atomic carbon with HCO^+ and $H_3{}^+$ respectively. The remaining reactions primarily display a power law relationship where the change in $C_{10}H_7CN$ abundance with respect to change in rate coefficient decreases at larger rate coefficient perturbations. The exceptions are the cosmic-ray ionization of H_2 and He, ranks 7 and 10 respectively, which show strong exponential decays and non-monotonic behavior in the case of H_2 ionization.

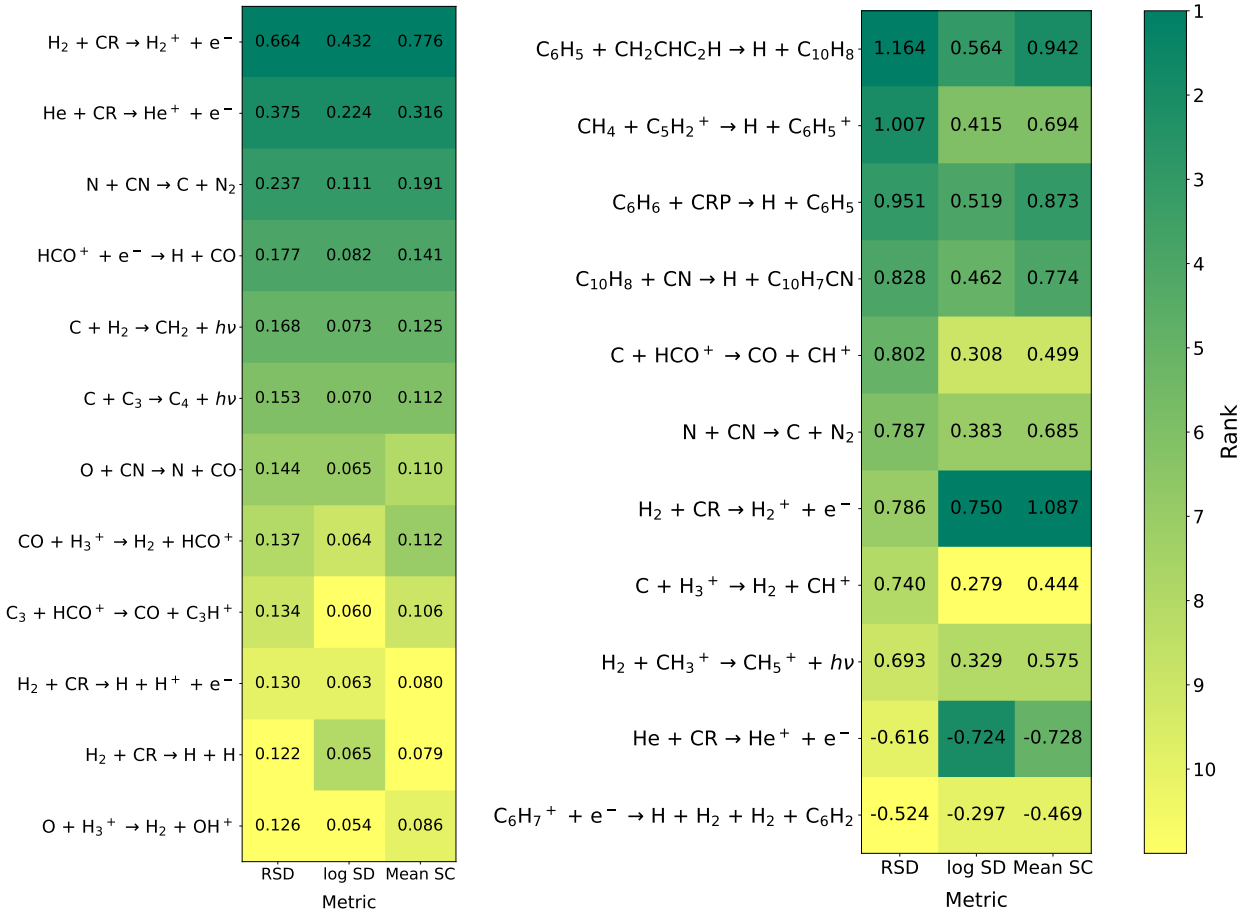

Figure S1: Heat map of key reactions according to the three OAT metrics at 541100 years for (left) the overall network and (right) $C_{10}H_7CN$ with a factor of 10 range in variation. All reaction within the top 10 with any of the three metrics are shown. The shading of each cell corresponds to the reaction's rank, with the exact sensitivity metric also given. Reactions ranked #11 or lower are given the lightest shading.

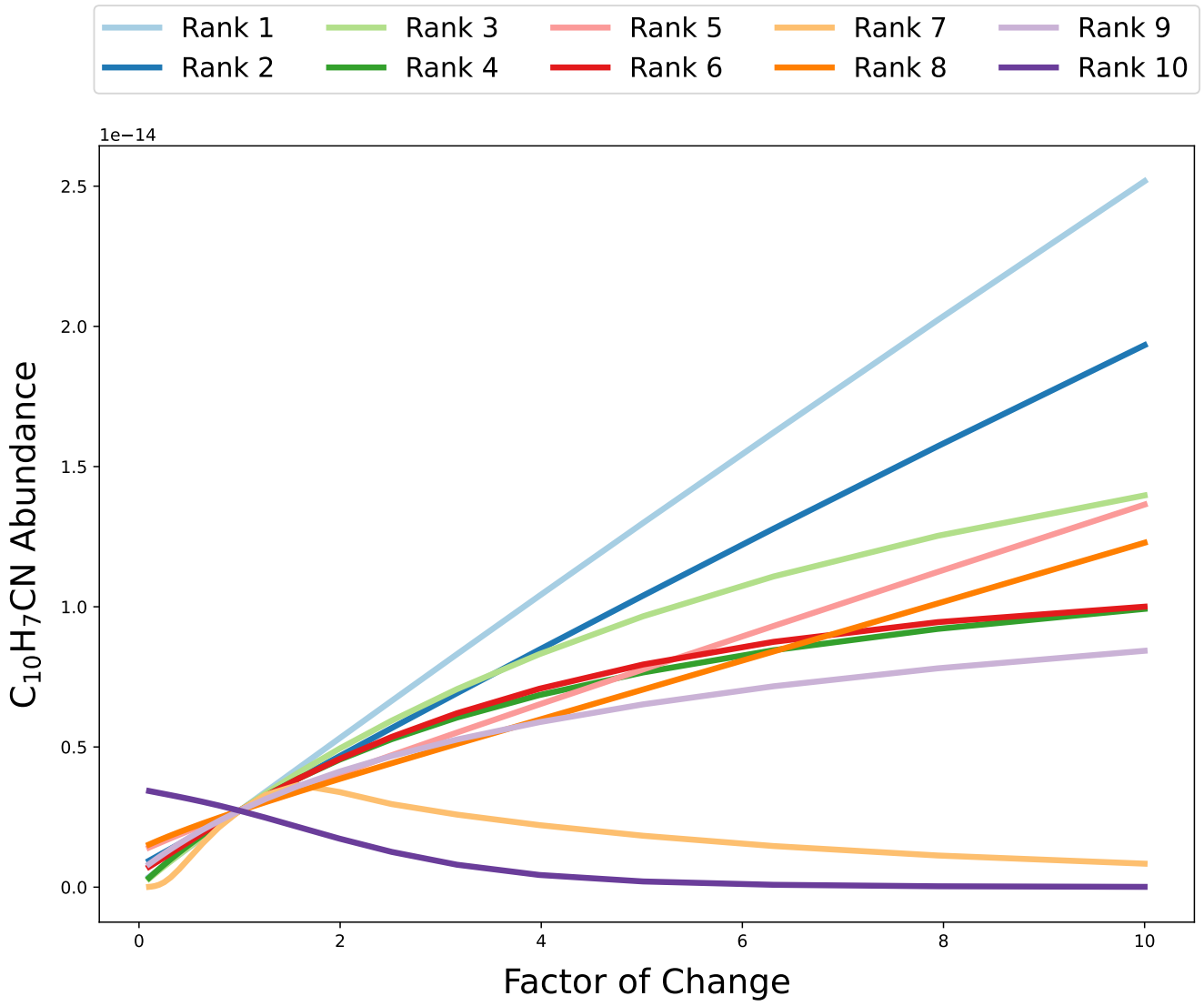

Figure S2: Abundances of $C_{10}H_7CN$ at 541100 years as a function of factor of change in rate constant for the top 10 reactions. Rankings are based on the RSD metric using the factor of 10 OAT data. Each curve represents one reaction.

S2: Convergence of Monte Carlo Results

In order to investigate the convergence of rank correlations coefficients, four analyses were performed on the same network with 5,000, 10,000, 15,000, and 20,000 iterations. For each analysis all reactions were ranked by average rank correlation coefficients. The differences in these ranks compared to those obtained from the one-at-a-time analysis are displayed in Figure S3 as a function of reaction rank. As these methods differ, both in definition of sensitivity as well as number of rate coefficients varied at once, non-zero rank differences are expected. However, this comparison does allow for the determination of when rank correlation coefficients become dominated by noise. This is evidenced by a sudden, large spike in rank difference, followed by consistently large rank differences indicating nearly maximum disagreement. As the number of iterations increases, the point at which this occurs gets pushed back slightly, from rank $\sim$50 for 5,000 iterations to rank $\sim$100 for 20,000 iterations. Likewise, a plot of average rank difference as a function of reaction shows that the steep increase in average rank difference occurs at later ranks when the number of iterations increases. It is clear that even 20,000 iterations is not enough for complete convergence due to the large number of reactions, and thus large parameter space. The key reactions are unaffected, but care should be taken with results beyond these.

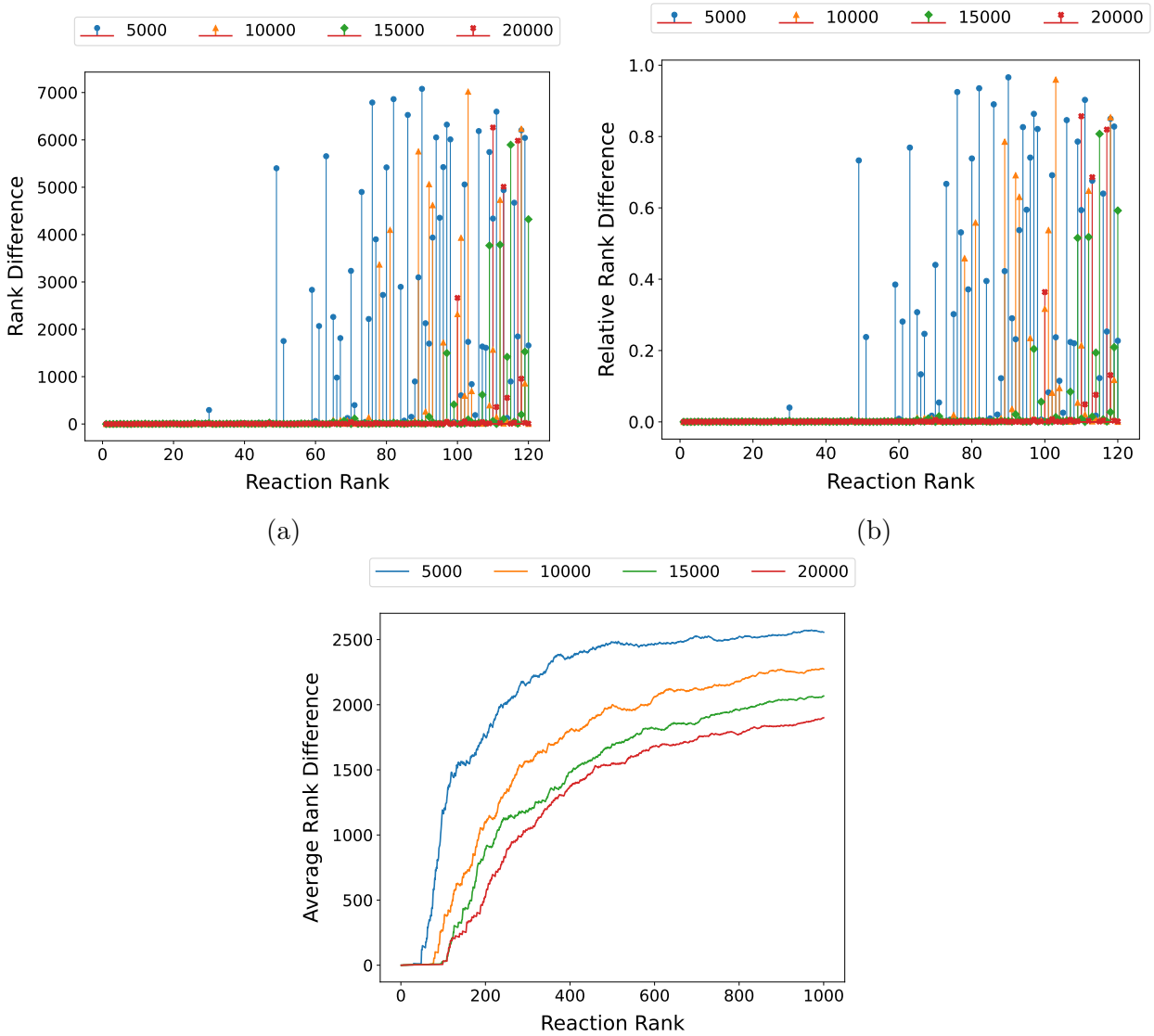

Figure S3: Difference in ranking between RSD and RCC metrics as a function of reaction rank, where each color represents a Monte Carlo analysis with some number of iterations. The top two plots are stem plots of the (a) absolute rank difference and (b) relative rank difference, ie. the absolute rank difference divided by the maximum possible rank difference at the given rank. In (c) the rolling average rank difference as a function of rank is plotted.

S3: Time Dependence of Key Intermediates

The key reactions for the overall network contain a number of processes that are important for "early-stage" hydrocarbon growth, while $C_{10}H_7CN$ is highly sensitive to many of these same reactions as well as a few directly involving aromatic species. Species such as C, HCO^+, CH_2, C_3 are important intermediates to hydrocarbon growth that appear in a number of these key reactions. Likewise, species such as CH_4 and C_6H_5 play major roles in the formation of large aromatic molecules such as $C_{10}H_7CN$. The abundances of these intermediate species in the nominal model are plotted as a function of time in Figure S4. C and CH_2 are most abundant before 10^5 years, after which there is a steep drop in atomic carbon abundance as it is rapidly converted into more complex species. Simpler hydrocarbons and carbon-chain species like CH_4 and C_3 reach their maximum abundances shortly after 10^5 years but display large abundances throughout the 10^5-10^6 years range. Large, complex hydrocarbons such as C_6H_5 do not achieve appreciable abundances until approximately 10^5 years, with maximum abundances not obtained until 5×10^5 years or later. HCO^+ does not show significant deviations in abundance between 10^5 and 10^6 years, consistent with its role as a major proton donor over this range of times.

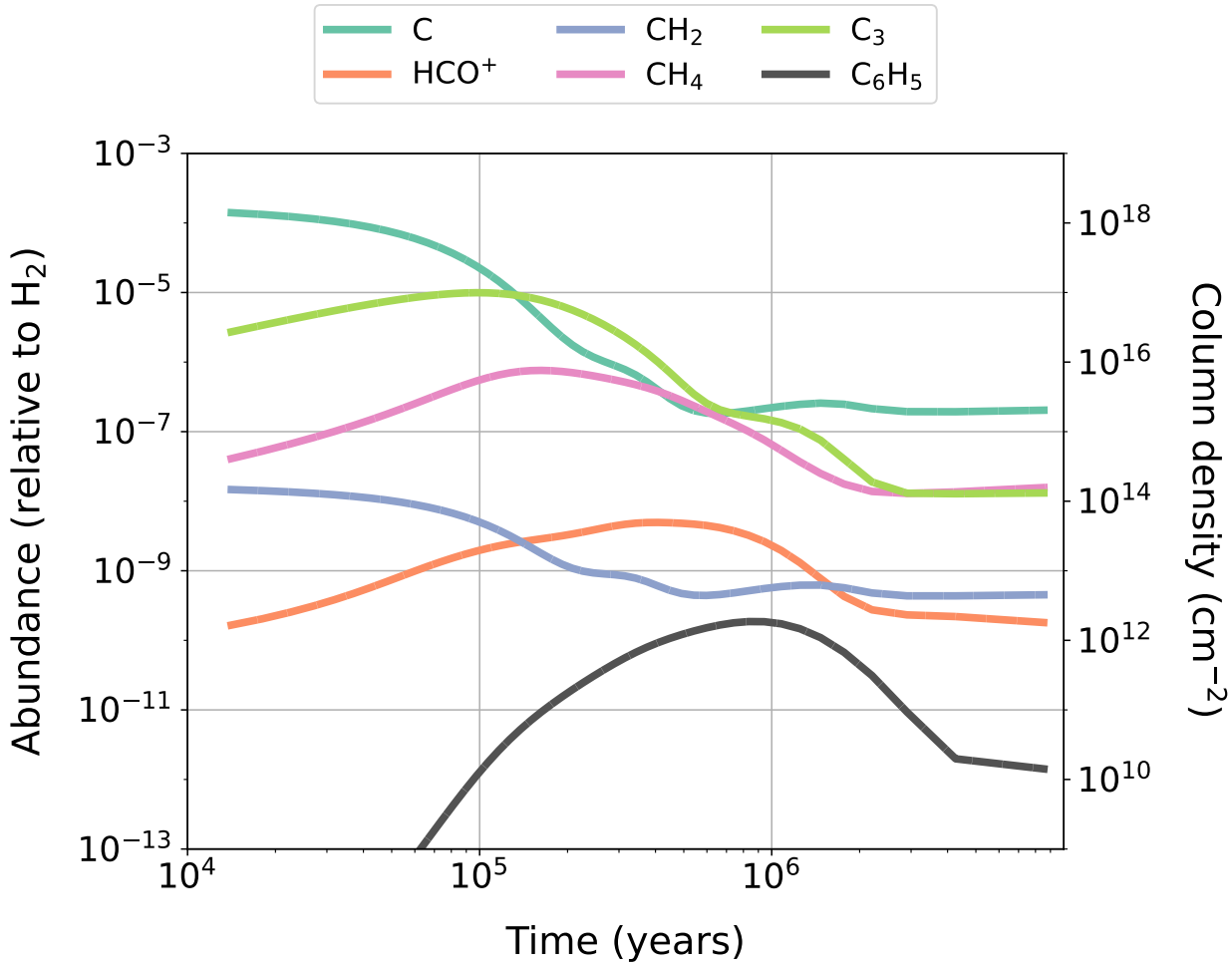

Figure S4: Modeled abundances with respect to H_2 as a function of time for select intermediate species identified as important to the overall network or $C_{10}H_7CN$ by the sensitivity analyses.

S4: Rate Coefficients of Key Reactions

Table 1 displays the rate coefficient information for the key reactions identified in Figures 3 and 6 of the main text. The `NAUTILUS` code uses three parameters to calculate rate coefficients at a given temperature. These parameters are given along with the corresponding rate coefficient at 10 K for each reaction. Reactions involving cosmic-ray processes, colored red, are calculated using the equation

$$k = \alpha\zeta, \tag{1}$$

where ζ is the cosmic-ray ionization rate (set to be $1.3 \times 10^{-17}\,\mathrm{s}^{-1}$ in our model) and α is a unitless prefactor. Reactions colored blue are ion-neutral processes with rate coefficients calculated using a Su-Chesnavich expression,

$$k = \alpha\beta\left(1 + 0.0967\gamma\left(\frac{300}{T}\right)^{1/2} + \frac{300\gamma^2}{10.526T}\right). \tag{2}$$

Here α is the branching ratio, β is the Langevin rate in units of $\mathrm{cm}^3\,\mathrm{s}^{-1}$, and γ is a unitless parameter that describes the temperature dependence based on the dipole moment and polarizability of the neutral species. The remaining reactions are calculated using a modified Arrhenius equation,

$$k = \alpha\,(T/300)^{\beta}\,e^{-\gamma/T}, \tag{3}$$

where α is the prefactor in units of $\mathrm{cm}^3\,\mathrm{s}^{-1}$, β is a unitless temperature dependence parameter, and γ is the activation energy in units of K.

Table 1: Key Reaction Rate Parameters

Reactions	α	β	γ	k (10 K)
$H_2 + CR \longrightarrow H_2^+ + e^-$	9.30×10^{-1}	0	0	1.21×10^{-17}
$C + H_2 \longrightarrow CH_2 + h\nu$	1.00×10^{-17}	0	0	1.00×10^{-17}
$C + C_3 \longrightarrow C_4 + h\nu$	4.00×10^{-14}	-1.00	0	1.20×10^{-12}
$C + CRP \longrightarrow C^+ + e^-$	1.02×10^{3}	0	0	1.33×10^{-14}
$He + CR \longrightarrow He^+ + e^-$	5.00×10^{-1}	0	0	6.50×10^{-18}
$C + CH_2 \longrightarrow H + CCH$	1.00×10^{-10}	0	0	1.00×10^{-10}
$C + H_3^+ \longrightarrow H_2 + CH^+$	2.00×10^{-9}	0	0	2.00×10^{-9}
$C + HCO^+ \longrightarrow CO + CH^+$	1.10×10^{-9}	0	0	1.10×10^{-9}
$HCO^+ + e^- \longrightarrow H + CO$	2.80×10^{-7}	-0.69	0	2.93×10^{-6}
$C + C_5 \longrightarrow C_3 + C_3$	1.50×10^{-10}	0	0	1.50×10^{-10}
$C_3 + HCO^+ \longrightarrow CO + C_3H^+$	1.40×10^{-9}	0	0	1.40×10^{-9}
$N + CN \longrightarrow C + N_2$	8.80×10^{-11}	0.42	0	2.11×10^{-11}
$O + CN \longrightarrow N + CO$	5.00×10^{-11}	0	0	5.00×10^{-11}
$CO + H_3^+ \longrightarrow H_2 + HCO^+$	9.45×10^{-1}	1.99×10^{-9}	0.251	2.47×10^{-9}
$HCNH^+ + e^- \longrightarrow H + HCN$	9.62×10^{-8}	-0.65	0	8.78×10^{-7}
$O + H_3^+ \longrightarrow H_2 + OH^+$	7.98×10^{-10}	-0.16	1.41	1.18×10^{-9}
$C_4 + e^- \longrightarrow C_4^- + h\nu$	1.10×10^{-8}	-0.50	0	6.02×10^{-8}
$C_6H_6 + CRP \longrightarrow H + C_6H_5$	2.93×10^{3}	0	0	3.80×10^{-14}
$C_{10}H_8 + CN \longrightarrow H + C_{10}H_7CN$	1.50×10^{-10}	0	0	1.50×10^{-10}
$C_6H_5 + CH_2CHC_2H \longrightarrow H + C_{10}H_8$	2.50×10^{-10}	0	0	2.50×10^{-10}
$CH_4 + C_5H_2^+ \longrightarrow H + C_6H_5^+$	8.00×10^{-10}	0	0	8.00×10^{-10}
$H_2 + CH_3^+ \longrightarrow CH_5^+ + h\nu$	3.78×10^{-16}	-2.30	21.5	1.10×10^{-13}
$H + CH \longrightarrow C + H_2$	1.24×10^{-10}	-0.26	0	5.12×10^{-11}
$C_6H_7^+ + e^- \longrightarrow H + H_2 + H_2 + C_6H_2$	2.00×10^{-7}	-0.83	0	3.37×10^{-6}